

Electronic Properties of Synthetic Shrimp Pathogens-derived DNA Schottky Diodes

Nastaran Rizan^{1,2,3}, Chan Yen Yew^{1,2,4}, Maryam Rajabpour Niknam^{1,2,5}, Jegenathan Krishnasamy¹, Subha Bhassu^{2,4}, Goh Zee Hong^{2,4}, Sridevi Devadas^{2,4}, Mohamed Shariff Mohd Din⁸, Hairul Anuar Tajuddin³, Rofina Yasmin Othman^{2,4}, Siew Moi Phang^{1,6}, Mitsumasa Iwamoto⁷ and Vengadesh Periasamy^{1*}

¹Low Dimensional Materials Research Centre (LDMRC), Department of Physics, Faculty of Science, University of Malaya, 50603 Kuala Lumpur, Malaysia

²Institute of Biological Sciences, Faculty of Science, University of Malaya, 50603 Kuala Lumpur, Malaysia

³Department of Chemistry, Faculty of Science, University of Malaya, 50603 Kuala Lumpur, Malaysia

⁴Centre for Research in Biotechnology for Agriculture (CEBAR), 50603 Kuala Lumpur

⁵HIR functional molecules laboratory, Institute of Biological Sciences, Faculty of Science, University of Malaya, 50603 Kuala Lumpur, Malaysia

⁶Institute of Ocean and Earth Sciences, University of Malaya, Kuala Lumpur 50603, Malaysia

⁷Department of Physical Electronics, Tokyo Institute of Technology, 2-12-1 Okayama, Meguro-ku, Tokyo 152-8552, Japan

⁸ Faculty of Veterinary Medicine, Universiti Putra Malaysia, 43400 Serdang, Selangor, Malaysia

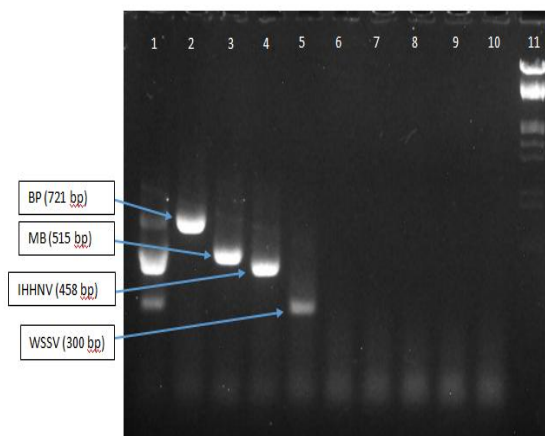
***Corresponding Author:** Associate Professor Dr. Vengadesh Periasamy, Low Dimensional Materials Research Centre (LDMRC), Department of Physics, Faculty of Science, University Malaya, Kuala Lumpur, Malaysia. Email: vengadeshp@um.edu.my, Tel: +60-379674038.

Supplementary 1

PCR detection emphasises the designed primers which targets the corresponding sequence. The above results show that the dual priming oligonucleotide (DPO) primers designed targeted on prawn and shrimp viruses. These patented primers were able to detect and differentiate the type of virus infection. A mixture of primers set allows simultaneous detection of 4 types of virus infections through band sizes. While in this paper, we emphasised in using DNA-specific Schottky diodes to generate I-V curve profiles in differentiating the types of virus infection. Different ATCG combination and nucleic acid sequence will generate different I-V curves which can be utilised to differentiate the type of infection. Our results indeed have been compared with the PCR result in generating reasonable data (I/V curve) in concluding the type of I/V curve versus type of infection.

PRAWN CHECKER – V1

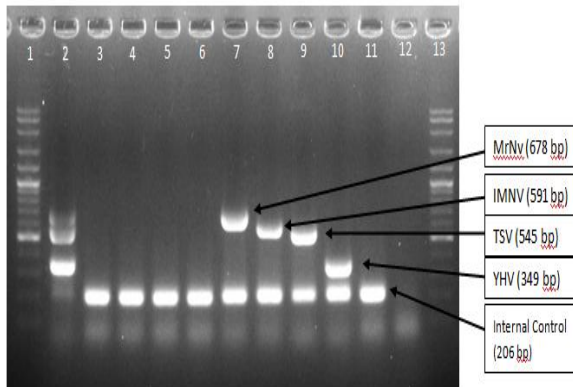
Detection using PRAWN CHECKER – V1 DNA viruses primer mix



Lane 1: The DNA 4plex result (4 target DNA viruses)
Lane 2: sample infected by BP virus
Lane 3: sample infected by MB virus
Lane 4: sample infected by IHNV virus
Lane 5: sample infected by WSSV virus
Lane 6: sample infected by MNV virus
Lane 7: sample infected by IMNV virus
Lane 8: sample infected by TSV virus
Lane 9: sample infected by YHV virus
Lane 10: NTC (No Template Control)
Lane 11: DNA marker

Figure S1. Multiplex of DNA viruses using DPO primers mixture. Lane 1 shows the multiplex bands of 4 multiplex DNA viruses while lane 2 to 5 shows individual bands of DNA viruses with different band size.

Detection using PRAWN CHECKER – V1 RNA viruses primer mix



Lane 1 and 13: DNA marker

Lane 2: The RNA 5plex result (4 target RNA viruses with sample cDNA)

Lane 3: cDNA of sample infected by BP virus

Lane 4: cDNA of sample infected by MB virus

Lane 5: cDNA of sample infected by IHNV virus

Lane 6: cDNA of sample infected by WSSV virus

Lane 7: cDNA of sample infected by MrNV virus

Lane 8: cDNA of sample infected by IMNV virus

Lane 9: cDNA of sample infected by TSV virus

Lane 10: cDNA of sample infected by YHV virus

Lane 11: cDNA of sample healthy sample

Lane 12: NTC (No Template Control)

Figure S2. Multiplex of RNA viruses using dual priming oligonucleotide (DPO) primers mixture. Lane 1 shows the multiplex bands of 4 multiplex RNA viruses while lane 7 to 10 shows individual bands of RNA viruses with different band size.

Supplementary 2

This new technique provides the potential to achieve sensitive and high-throughput species identifications. The simplicity nature of these methods is suitable for the development of a hand-held DNA diagnostic device. The following steps were undertaken to demonstrate the reproducibility and sensitivity of the electronic sensor;

Please refer to the Supplementary Figure below, which explains the positive biased I-V profiles for different concentrations of DNA AHPND (from about 300 ng/ul to 5 ng/ul).

In this technique, we prepared different concentrations of DNA strands to investigate the sensitivity of the sensor operation. Extensive experiments (more than 50 repetitions each) were carried-out to obtain data from different concentrations of DNA (high to lowest levels) to proof the sensitivity of this electronic sensor.

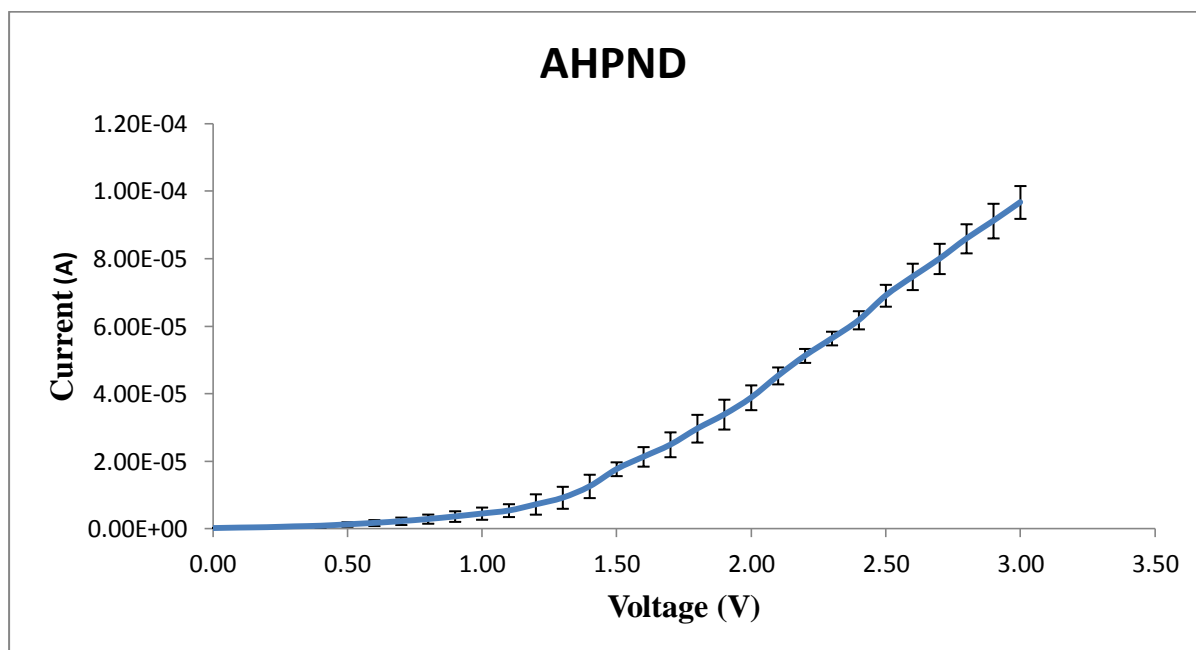


Figure S3: Positive biased I-V profiles for different concentrations of DNA AHPND (from about 300 ng/ul to 5 ng/ul). The small error bars indicate the high repeatability and sensitivity of the experiments carried-out.

Supplementary 3

Please refer to the Supplementary data below, which shows real sequences of our samples

Sequences of viral gene

Infectious hypodermal and hematopoietic necrosis virus (IHHNV) (987bp)

```
ATGTGCGCCG ATTCAACAAG ATCAAGCCCA AGGAAAAGAT CCAGGAGGGA
TGCACATAAT GAAGACGAAG AACACGCCGA GGGATCAAGT GGACCAGACC
CACACAGATG TCTACAATTC AATACGGGAG ACTCAATACA TATTACTTTC
CAAACAAGAA GATACTTCGA ATTCGACGCT GCCAATGATG GAAACTTCGA
CGGAAAAAAC TTATACTGCC TCCCCTACA TTGGATGAAC TTATATCTCT
ATGGACTAAA AAGCAGTGAC AGTTCAGCAA CAGAAACACA GCGATATAAG
ATGGTAAAGT CAATGATGAA AACCTACGGA TGGAAAGTTC ACAAAGCAGG
CGTCGTAATG CACTCAATGG TACCCCTTAT GAAAGACTTA AAGGTATCAG
GAGGAACATC ATTTGAAACT CTCACATTTA CAGATACCCC ATATTTAGAA
ATATTTAAGG ATACTACTGG ACTACATAAT CAACTAGCAA CTAAGGAAGC
CGACGTAACA TTAGCAAAT GGATACAAAA TCCGCAACTT GTGACAGTAC
AATCAACAGC AGCAAATTAT GAAGACCCAA TCCAACAATT TGGATTTATG
GAACAAATGC GAACTGGAGA CCGAAAAGCC TATACAATCC ATGGTGACAC
TAGAAACTGG TATGGCGGAG AAATACCAAC AACCGGACCC ACGTTCATCC
CAAAATGGGG TGGCCAAATG AAGTGGGACA AACCAAGCAT TGGAAACCTA
GTCTACCCAG CGGATCACCA TACAAACGAC TGGCAACAAA TCTTCATGAG
AATGTCACCA ATCAAAGGAC CAAATGGAGA CGAACTTAAA CTTGGCTGCA
GAGTACAAGC CGACTTCTTC CTCAACCTAG AAGTACGACT CCCACCACAA
GGATGTGTCT CAAGTTTGGG AATGTTACAA TATCTTCACG TACCATCTAC
TGGACAACCT AACAGATGTT ATATTATGCA TACTAAC
```

Monodon baculovirus (MBV) (600bp)

```
ATGTTTCGACG ATAGCATGAT GATGGAAAAT ATGGACGACC TTAGTGGAGA
TCAGAAGATG GTGCTCACAC TTGCTGCGGC TGGTGCTGTG GCTGGAGCAT
CGAAGATGTT GAACGAAGCT GCAGACCTGA AGAAAAATTA CAAGGATACT
CCACTTGAAG AATATTTCAA AGATAAGTAT TCAGGCAACA AAAAAAGAAA
GATCACTGAT CAGGAATTTG AACTCCCTAA GTCTATTGAT CCACTTGAAA
ATCATTTCAA AGGACTGTCC CGTCCTCGTG TAGGCCCTCG AATGGCAAAA
CAGCTTGCAA ATAAAATGAG TGACAACAAA ATGCATTATA AATTTAACAG
CTTTCAGACA AATAAACACT TTAATACTCA CACAATTTAC AAGCGAACAA
ATCTCACTTC TTCTAAACTA ATGGGCTTTT CGGGTCAGAG TGATTTTGGC
GTACCCAAAT ACAACAGTGC AGTCACACTT CCTCTGGAAG TATTGGAATT
TTGGGTAGGT GACAACACAA ATCCTAATGT TGAACATTCT AAGGGTAGTA
TGGCATTGAA AAATAGTGAA TGTATGATTG CATCTATGAA ACTTAAACTT
```

Taura syndrome virus (TSV) (900bp)

AACATCAAAC TATATGGGCA TGCCCCATCT GTGACATCTT CAGTATATCC
GTCTACTCAG TCCGGATATG ATGATGATTG TCCCATTGTG CATGCGGGAA
CTGATGAGGA TTCTTCTAAA CAGGGGATTG TCTCAAGGGT TGCAGACACC
GTTGGTGCGG TGGCAAATGT AGTAGATGGG GTAGGAGTAC CTATTCTATC
CACAATTGCC AAGCCTGTTT CCTGGGTGTC GGGCGTAGTG AGTAATGTAG
CTTCAATGTT CGGATTTTCA AAAGATAGGG ATATGACGAA AGTCAACGCA
TATGAGAACT TACCTGGTAA GGGCTTCACT CATGGTGTTG GCTTCGATTA
TGGCGTACCC CTGTCTCTTT TCCCTAACAA TGCCATTGAT CCCACAATTG
CAGTGTCTGA AGGATTAGAT GAAATGTCTA TTGAATACCT AGCACAGCGA
CCATATATGC TCAACAGATA CACTATCAGA GGTGGTGACA CTCCTGATGA
ACATGGAACA ATTATTGCAG ATATTCCAGT GAGTCCTGTC AATTTTAGTT
TGTATGGTAA AGTTATTGCT AAGTATCGCA CCCTATTCGC TGCCCCAGTT
AGTCTAGCTG TAGCAATGGC TAATTGGTGG CGTGGAAATA TTAACCTTAA
TCTTCGCTTT GCTAAGACGC AGTACCATCA ATGCAGATTG CTGGTGCAAT
ATCTCCCCTA TGGTAGTGGT GTTCAACCAA TAGAAAGTAT CCTTTCACAG
ATCATCGACA TCTCACAAGT CGATGATAAG GGTATTGACA TTGCTTTTCC
TTCCGTCTAT CCCAATAAGT GGATGCGAGT GTACGATCCA GCGAAAGTTG
GGTACACGGC AGATTGTGCC CCAGGCCGAA TCGTCATTTT CGTTCTCAAC

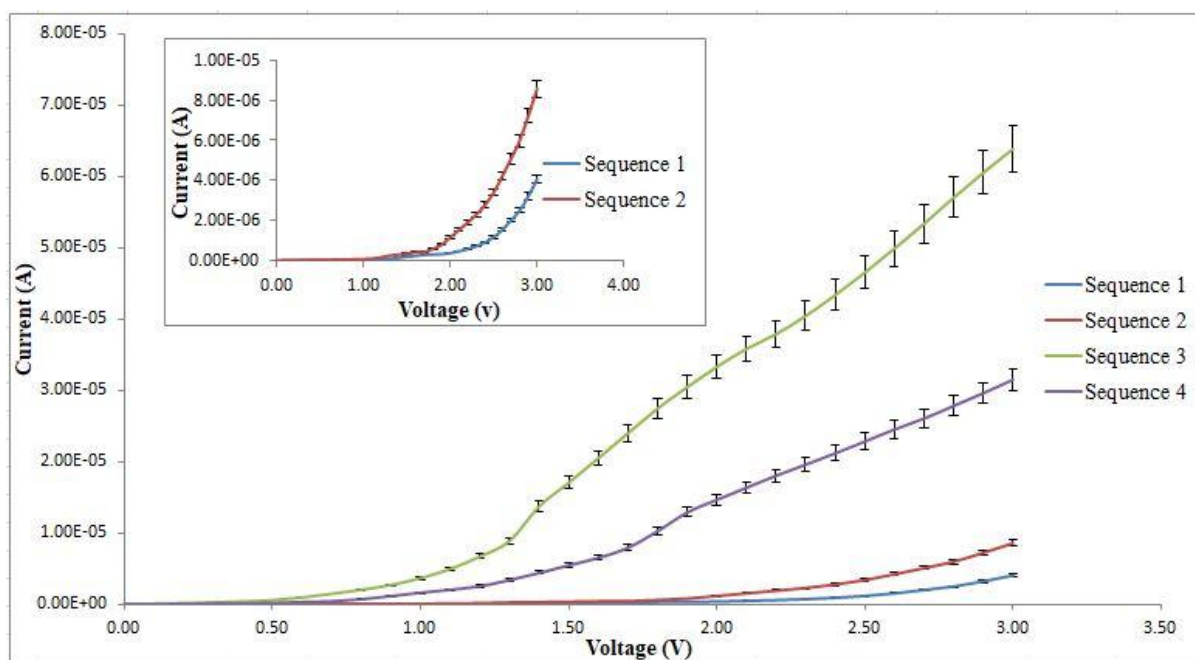
Yellowhead virus(YHV) (684bp)

ATGAACCGTC GTACACGCAC CGCAACTCCT ATGCCTCGTC GTCGCCTACC
TCCTTCCAAC CGACTCACTC GCAATGCAAG GCTCATCGAG ATTCCTCAAT
CCTTCGCAGT CGAACGCGGA AATGGATGGA TGTTGGCATA TGCCCCAGGT
AAAAATCCAC TACCGGGAAA AGTCATCGCT CGTATGCAGG CATCTCCATT
CATTCAAGGA CTCAAGAAC AATCCCTCCA AGTTGTCAAG TCATCTGATG
GTAAGTATTC AATTTCAAAG AGATACGGTA AAATGGCCAT CACCTATCTT
AATCCCAACG ATCCCATCTT GCCAAAGCGT TCAACACAGA AGTCAATCGT
TCCCGATCCT TCCCTTGACA TAGAGAACCT AGCTGAAGGT ATCCACGCAA
TGAGCCTTGA AGACGACGAA CCCATGGAAA CACAATCA

Supplementary 4

The electronic method employed in this work is highly accurate and will strongly depend on the electronic pathway presented to regarding the resistance pathway provided by the base sequence. Due to the nature of current conduction mechanism, it is well understood that conductivity signature will only be influenced by the “least resistance” pathway which will strongly be dependent on both the base sequence and number of base pair. In this context, it is understood that with different base sequences but with a same number of base pairs, each of the 2 DNA sequences demonstrate characteristic or fingerprinting electronic profiles unique to their charge pathway mechanism.

However, we still carried-out the necessary experiment to demonstrate the variations that arise even within different DNA sequences but with the same number of base pairs shown below; please refer to the supplementary Figure below:



S4: Four sets of complementary strands of DNA with a length of 20bp were designed, synthesized and subjected IV characterization. Each set had a different sequence. Sequence 1 is rich in GC bases (GC=70%), sequence 2 is rich in AT bases (GC= 25%) while sequence 3 and sequence 4 have same GC bases (GC=50%). These sequences exhibited different electronic profile.

Sequence 1

5' GCA TTC GGC GCG GCG TAA CG 3'
3' CGT AAG CCG CGC CGC ATT GC 5'

Sequence 2

5' ATA CCT GTC AGA AAT TAA TA 3'
3' TAT GGA CAG TCT TTA ATT AT 5'

Sequence 3

5' GCA TGA TCC CTG ACT ATG TC 3'
3' CGT ACT AGG GAC TGA TAC AT 5'

Sequence 4

5' TAA GCA CGT CTG ACC ATG TC 3'
3' ATT CGT GCA GAC TGG TAC AG 5'